

## Observation of fast positron diffraction from a Si(111)7x7 surface

A. Kawasuso, Y. Fukaya, K. Hayashi, M. Maekawa, T. Ishimoto, S. Okada  
and A. Ichimiya

Advanced Science Research Center, Japan Atomic Energy Research Institute  
1233, Watanuki, Takasaki, Gunma, 370-1292 JAPAN  
ak@taka.jaeri.go.jp

**Keywords:** Positron diffraction, Total reflection, Surface, Si(111)7x7

**Abstract.** In this article we present the first observation of high-energy positron diffraction from a clean Si(111)7x7 surface. A 20 keV positron beam with a sufficient coherence length was reflected at the surface and a diffraction pattern was observed. The fractional order Laue zones, which were assigned to be the 1/7-th, 2/7-th and 3/7-th orders from the kinematical consideration were well seen. The rocking curve (diffraction intensity versus glancing angle plot) was also measured. In the total reflection region of the rocking curve, the intensity distribution was hardly reproduced when adopting the distance between the adatom and stacking fault layers and also the damping potential due to the electronic excitation determined previously. Possible reasons are discussed.

### Introduction

One advantage of high-energy positron diffraction method is the appearance of the total reflection below a critical glancing angle of incidence [1]. This is due to the positive crystal potentials for positrons. In the total reflection mode, the reflected positrons convey information from the topmost surface with fewer disturbances from its interior. Total reflection is not observed in the case of electron diffraction. X-ray total reflection is possible. The characteristic differences between positrons and X-rays are, however, their penetration depths and strength of reflection. Positrons survey a very shallow region (a few Å), while the typical penetration depth of X-rays is ~100 Å even in the total reflection mode. The scattering cross section of positrons from atoms is more than three orders of magnitude greater than that of X-rays. Thus, for the surface sensitivity, the total reflection positron diffraction is superior.

It is well known that Si exhibits unique surface reconstruction and phase transition. The 7x7 reconstruction phase is stable below 850 °C. The surface structure was determined from the direct observation by the scanning tunneling microscopy (STM) and Patterson analysis of the transmission electron diffraction pattern [2,3]. These days, the dimer-adatom-stacking fault (DAS) structure is the most widely accepted model for the Si(111)7x7 surface [3]. The interlayer distances of the DAS structure were determined by low energy electron diffraction (LEED) [4], reflection high-energy electron diffraction (RHEED) [5,6] and X-ray diffraction (XRD) [7]. The interlayer distances determined by the former two are consistent with the theoretical prediction [8] within an error of 0.1 Å. However, the distance between the adatom and stacking fault layer determined by the XRD is remarkably larger than all the other data. Although the precise determination of the interlayer distances is important when considering the thermal vibration of adatoms and adsorption potential on the Si(111)7x7 surface. The above discrepancy has long been unsolved.

In this work, we report the observation of the diffraction pattern from the clean Si(111)7x7 surface. The rocking curve was also measured and analyzed using the dynamical diffraction theory to extract the precise vertical position of adatoms and to terminate the above controversy.

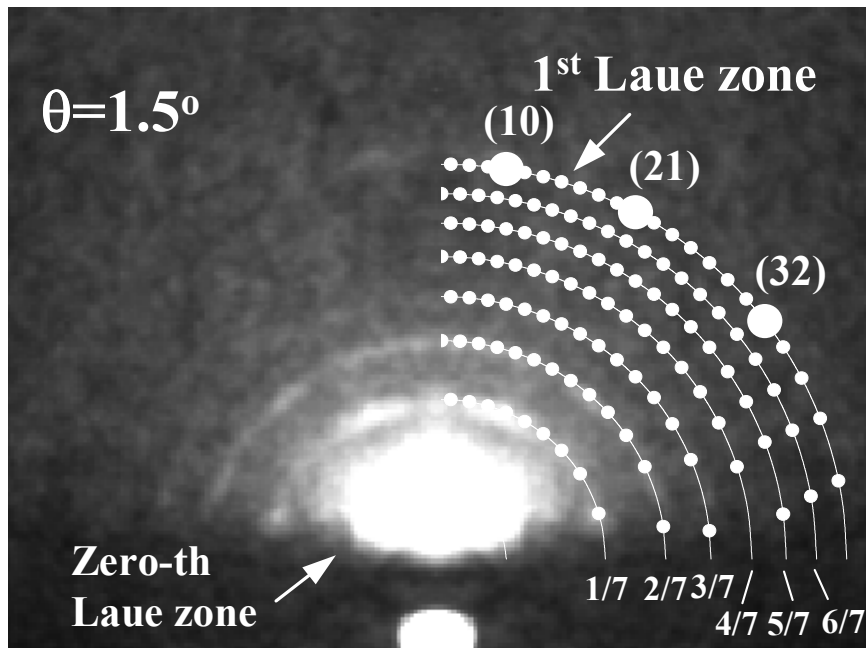


Fig. 1 Reflection high-energy positron diffraction pattern from a clean Si(111)7x7 surface at the  $[11\bar{2}]$  incidence and at a glancing angle of  $1.5^\circ$ . Spot positions expected from the reciprocal lattice are also drawn in the right half part of the figure.

### Instrumentation and Experiment

A 20 keV well-collimated positron beam was generated by the electrostatic apparatus described elsewhere [9,10]. A positron source with an activity of 217 MBq and an active diameter of 5 mm was installed in the positron gun part. The source was electrically floated at 20 kV. The fast positrons were moderated using a well-annealed tungsten single crystal with a thickness of 500 nm. The slow positrons were extracted from the moderator using a grid electrode with a relative bias potential of -0.4 kV. Then, the positron beam is focused by the Wehnelt, Soa and anode electrodes. The bias potential of the anode electrode was set to be 19.2 kV and those for the former two electrodes were adjusted between 19.6 kV and 19.2 kV. The above positron gun was realized by the Brandeis research group [11]. Three unipotential lenses were installed after the anode exit. To prevent the direct fly of non-thermal positrons, a hemispherical type electrostatic analyzer with a bent angle of  $45^\circ$  was fabricated. Then, the positron beam was further transported using two unipotential lenses. Finally, the beam was deflected downward by  $2.8^\circ$  and collimated to 1 mm diameter using a long pinhole slit (100 mm length). Although the beam flux was rather weak ( $2 \times 10^3$  e<sup>+</sup>/s), the energy dispersion and the angular spread were reduced to less than 0.1 % and  $0.1^\circ$ , respectively. So far, the goodness of a beam is expressed in terms of the brightness per volt. Referring to the expression of Brandes [12], the present brightness per volt is estimated to be approximately  $\sim 10^6$  e<sup>+</sup>/s/cm<sup>2</sup>/rad<sup>2</sup>/V, which is more or less comparable to the case employing the brightness enhancement technique. Thus, we may not set up the re-moderation stage as long as the restriction from the Liouville's theorem is reduced by accelerating positrons.

Instead of the brightness per volt, we have to import a concept of coherence length, which is used as the goodness of a beam in diffraction experiments, as follows [13]. Any beams have energy spreads ( $\Delta E$ ). Therefore, the incident beam should be described as a wave packet and not as a plane wave. This means that the beam has a finite wave length. If the size of the surface unit cell is larger than the wavelength, the surface super structure is hardly observed as fractional order spots. The probability amplitude of the plane wave is uniform everywhere and thus there are no limitations in the observable unit cell size. The coherence length in the surface parallel direction is given by  $l_p = 2\pi/\Delta k = 24.5E^{1/2}/\Delta E$ , where  $\Delta k$  is the spread of the wave number. Due to a similar reason, the angular divergence of the

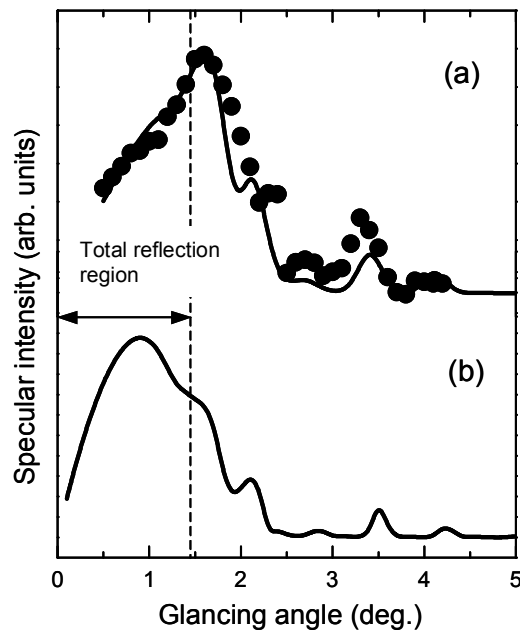


Fig.2 (a) Filled circle represents the experimental rocking curve of specularly reflected positrons obtained from the clean Si(111)7x7 surface at the one-beam condition ( $7.5^\circ$ -off oriented from the  $[11\bar{2}]$  direction). Solid line is the best theoretical rocking curve to reproduce the experiment. (b) Rocking curve for Si(111)7x7 surface obtained from theoretical calculation considering the atomic configurations and absorption potentials determined the previous RHEED study.

beam ( $\Delta\theta$ ) regulates the coherence length to the surface vertical direction:  $l_v = 12.3/\Delta\theta/E^{1/2}$ . A typical example to test the coherence length of the beam is the Si(111)7x7 surface which has seven times greater lattice constant ( $=3.84 \text{ \AA} \times 7 \sim 30 \text{ \AA}$ ) as compared to the bulk truncated surface. Thus, to observe the Si-7x7 surface the energy spread be reduced to less than  $\sim 100\text{eV}$  when  $E=20 \text{ keV}$ .

The sample used in this study was phosphorus-doped n-type Si(111) with a dimension of  $15 \times 5 \times 0.5\text{mm}$  and a resistivity of  $10 \text{ \Omega cm}$ . After surface cleaning with an acetone and ultra-pure water, the sample was transferred into a vacuum chamber evacuated to a base pressure of  $5 \times 10^{-8} \text{ Pa}$ . The sample flashing was taken place by the direct current flow for a short second and by cooling slowly to avoid the surface defect formation. A  $20 \text{ keV}$  positron beam was reflected at the surface at a glancing angle of  $0.5\text{-}4.2^\circ$ . Reflected positrons were observed using the microchannel plate assembly with a phosphor plane (Hamamatsu F2226-24P). Phosphor plane images were digitally accumulated until adequate brightness was achieved.

## Results and discussion

Figure 1 shows the diffraction pattern obtained at  $\theta=1.5^\circ$  and at  $[11\bar{2}]$  incidence. This glancing angle nearly satisfies the condition of the first Bragg reflection. Three fractional order diffraction patterns are seen between the zero-th and first Laue zones. To confirm these diffraction patterns are related to the  $7 \times 7$  reconstructed Si(111) surface the spot positions expected from the kinematical consideration are also drawn in the figure. From this, the patterns are explicitly attributed  $1/7$ -th to  $3/7$ -th Laue zones. Although individual spots are not well separated because of the limitation of the MCPA resolution, it is seen that the spot intensity varies in the same Laue zone. To interpret this feature, a full dynamical calculation is now under consideration. The other fractional order Laue zones, i.e.,  $4/7$ -th to  $6/7$ -th, are unfortunately not clearly seen. This is probably due to inadequate signal-to-noise ratio. The further attempts should be made to observe weak this diffraction pattern. The intensities of the fractional order patterns rapidly decreased with increasing the glancing angle. At  $\theta=4.0^\circ$ , these were not visible.

Figure 2 shows the rocking curve of the specularly reflected positrons in the one beam condition (incident direction is  $7.5^\circ$ -off oriented from the  $[11\bar{2}]$  direction). The intensity monotonically increases from  $\theta=0.5^\circ$  and reaches a maximum at  $\theta=1.6^\circ$ . Three peaks are seen at  $\theta=2.2^\circ$ ,  $2.7^\circ$  and  $3.4^\circ$ . The critical angle of total reflection is given by  $\theta = \arcsin(V_0/E)^{1/2}$ , where  $V_0$  is the average crystal

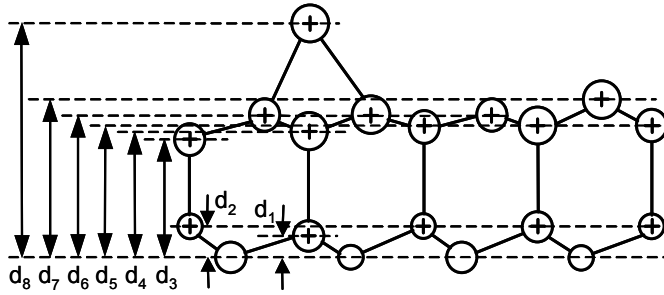


Fig. 3 Definition of interlayer distances of Si(111)7x7 surface.

potential. Taking  $V_0=12$  eV, the critical angle of total reflection is  $\theta=1.4^\circ$ . The Bragg condition is given by  $E\sin^2\theta=37.5n^2/d^2+V_0$  ( $n$ : integer,  $d$ : bilayer distance  $=3.14$  Å). Thus, the region up to  $1.4^\circ$  corresponds to total reflection. The peaks at  $1.6^\circ$ ,  $2.2^\circ$ ,  $2.7^\circ$  and  $3.4^\circ$  are assigned to the (111), (222), (333) and (444) Bragg reflections, respectively. The intensity distribution at  $\theta<1.8^\circ$  reflects the condition of the topmost surface. No major intensity losses and dip structures are found below  $1.6^\circ$ . This indicates that the surface is atomically smooth. However, the slope of the curve changes at around  $1.1^\circ$ . This small discontinuity might be arising from the adatoms.

We attempted to reproduce the experimental rocking curve based on the dynamical calculation [14] and to extract the vertical position of adatoms. In the calculation, the crystal potential is expressed as a complex potential ( $=V_0+iV''$ ). The imaginary part describes the absorption through the inelastic processes, which is composed of terms related to phonon scattering ( $V_{ph}$ ) and the electronic excitation ( $V_{el}$ ). Thermal vibration of atoms is represented by the Debye-Waller factor. The layer sequences in the DAS structure are assumed as shown in Fig. 3. At first, the rocking curves of specularly reflected positrons were calculated using the atomic configurations and absorption potential determined in the RHEED study [5]. Figure 2 (b) shows the rocking curve calculated using the same conditions as the RHEED study. It is readily seen that the calculation is compatible to the experiment at  $\theta>2.0^\circ$  but not in the total reflection region and around the first Bragg peak ( $\sim 1.6^\circ$ ). This is because in the RHEED the calculation conditions are optimized so as to reproduce the features of the higher order Bragg reflections. To reproduce the experimental rocking curve, the interlayer distances, the absorption potential and the Debye-Waller factor used in the RHEED study should be modified. During the preliminary calculations, we found that the rocking curve is quite sensitive to the relative distance between adatom and stacking fault layers ( $d_{ad}=d_8-d_6$ ). It is also found that the changes of the Debye-Waller factor and  $V_{ph}$  have only minor effects on the curve shape in the total reflection region. Thus, the distance between the adatom and stacking fault layers and the absorption potential due to electronic excitations ( $V_{el}$ ) are varied so as to reproduce the experimental rocking curve. The Debye-Waller factor and  $V_{ph}$  are fixed at  $0.3$  Å<sup>2</sup> and  $0.2$  eV, respectively. The solid line in Fig. 2 (a) is the calculated best rocking curve. The optimum distance between adatom and stacking fault layers was determined to be  $d_{ad}=1.52$  Å. Also, we obtained  $V_{el}=0.25$  eV. The Pendry R-factor is estimated to be  $0.17$  suggesting that the experimental curve is well reproduced.

Table 1 lists the  $d_{ad}$  values obtained in the present and previous studies. Early electron diffraction studies suggest  $d_{ad}=1.23$ - $1.28$  Å [4,5], which is comparable to the result from the first principles calculation ( $d_{ad}=1.34$  Å) [8]. Recent refined RHEED study [6] reported a greater value ( $d_{ad}=1.44$  Å). The XRD study gives a remarkably high value ( $d_{ad}=1.58$  Å) [7]. The present value ( $d_{ad}=1.52$  Å) is in the middle between these values. It has long been thought that the XRD overestimated  $d_{ad}$ . However, the above results indicate that  $d_{ad}$  determined in the XRD study is not necessarily unrealistic. Thus, the distance of the adatom and stacking fault layers should be around  $1.5$  Å. The first principles calculations underestimate  $d_{ad}$  and hence the improvement of the theory is needed.

The absorption potential due to the electronic excitation obtained above is approximately a half of that anticipated from the RHEED study [5] and a theory considering the bulk plasmon excitation [15]. Since the cross section of plasmon excitation itself should be quite similar for electrons and positrons, the smaller absorption potential may be interpreted as a lack of bulk plasmon excitation due to

Table 1 Mean distance between adatom and stacking fault layers ( $d_{ad}$ ) determined in the present and previous studies.

Present	XRD [7]	RHEED [5,6]	LEED [4]	Theory [8]
1.52 Å	1.58 Å	1.28 Å, 1.44 Å	1.23 Å	1.34 Å

incident positrons. Probably, incident positrons are reflected mostly at the topmost surface and hence the surface plasmon excitation with a smaller energy may be more efficient as compared to the bulk plasmon excitation.

### Summary

We have confirmed the observation of high energy positron diffraction from a Si(111)7x7 surface. The rocking curve for the specular beam was determined in the one-beam condition. It was found that the intensity distribution of totally reflected positrons was sensitive to the vertical position of adatom layer and to the electronic absorption potential. From the comparison between the experiment and a dynamical calculation, it was found that the adatom layer undergoes a greater outward relaxation than that expected from the first principles calculation. The distance between an adatom and the first layers can be determined precisely by the total reflection positron diffraction and XRD techniques, while the shift of interlayer distances in the sub-surface region (several atomic layers) by RHEED and LEED. Through complementary study it is anticipated that some important phenomena such as surface melting and phase transitions will be fully understood.

### References

- [1] A. Ichimiya, Solid State Commun. **28&29** (1992)143.
- [2] G. Binnig, H. Rohrer, Ch. Gerber, and E. Weibel, Phys. Rev. Lett. **50** (1983)120.
- [3] K. Takayanagi, Y. Tanishiro, S. Takahashi, and M. Takahashi, Surf. Sci. **164**(1985)367.
- [4] H. Huang, S. Y. Tong, W. E. Packard, and M. B. Webb, Phys. Lett. A **130**(1988)166.
- [5] A. Ichimiya, Surf. Sci. **192**, L893 (1987).
- [6] Y. Fukaya, K. Nakamura, and Y. Shigeta, J. Vac. Sci. Technol. A **18**(2000)968.
- [7] I. K. Robinson and E. Vlieg, Surf. Sci. **261**(1992)123.
- [8] Karl D. Brommer, M. Needels, B. E. Larson, and J. D. Joannopoulos, Phys. Rev. Lett. **68** (1992)1355.
- [9] A. Kawasuso, S. Okada, and A. Ichimiya, Nucl. Instrum. Methods Phys. Res. B **171**(2000)219.
- [10] T. Ishimoto, A. Kawasuso, and H. Itoh, Appl. Surf. Sci. **194**(2002)43.
- [11] K. F. Canter, P. H. Lippel, W. S. Crane and A. P. Mills, Jr., in: Positron Studies of Solids, Surfaces, and Atoms, eds. A. P. Mills, Jr., W. S. Crane and K. F. Canter (World Scientific, Singapore, 1986) p. 199.
- [12] G. R. Brandes, K. F. Canter, T. N. Horsky, P. H. Lippel and A. P. Mills, J. Phys. Condens. Matter **1**(1989)SA135.
- [13] G. Comsa, Surf. Sci. **81**(1979)57.
- [14] A. Ichimiya, Jpn. J. Appl. Phys., Part 2, **22**(1983)176.
- [15] G. Radi, Acata Cryst. A **26**(1970)41.

**Positron Annihilation - ICPA-13**

10.4028/www.scientific.net/MSF.445-446

**Observation of Fast Positron Diffraction from a Si(111)7x7 Surface**

10.4028/www.scientific.net/MSF.445-446.385

**DOI References**

[5] A. Ichimiya, Surf. Sci. 192, L893 (1987).

10.1016/0167-2584(87)90792-4